Metabolic Dysfunction Associated With Alterations in Gut Microbiota in Adolescents With Obesity

Alessandra Granato,[1] Quin Yuhui Xie,[1,2] Anthony Wong,[1] Christopher Yau,[1,3] Rebecca Noseworthy,[4] Tina Chen,[5] Connor Gianetto-Hill,[6] Emma Allen-Vercoe,[6] Cynthia J. Guidos,[3,5] Jill K. Hamilton,[4] and Jayne S. Danska[1,2,3]

Diabetes 2025;74:720–733 | https://doi.org/10.2337/db24-0866

Obesity in childhood is associated with adulthood obesity, type 2 diabetes (T2D), and future metabolic complications. The gut microbiota is a modifier of host metabolic function with altered bacterial composition associated with disease risk. Few studies have investigated the relationships among metabolic disease, inflammation, and the gut microbiota in youth, in whom these connections likely originate. Here, we characterized the gut microbiome of a cohort of 56 adolescents with obesity and without diabetes using fecal DNA sequencing with absolute bacterial quantitation together with immune and metabolic profiling. We observed multi–log order variation in absolute bacterial biomass dependent on host environment and associated with bacterial taxonomic composition based on a nested case-control comparison. Participants with higher biomass displayed a healthier phenotype with higher gut microbiome diversity; lower abundance of taxa associated with inflammation and pathogenicity, such as *Escherichia coli*; and lower levels of neutrophil activities. Further association analysis revealed sex-dependent variation, with higher levels of insulin resistance, fasting triglycerides, and markers of neutrophil activities in male adolescents with lower bacterial biomass. Together, these results suggest that intestinal bacterial biomass and composition are associated with metabolic and inflammatory dysregulation evident before T2D diagnosis and identify sex differences in microbiome-associated metabolic dysfunction in adolescents with obesity.

ARTICLE HIGHLIGHTS

- Previous obesity studies of the gut microbiome have focused on adults. Childhood obesity rates have risen substantially and confer elevated T2D risk. We investigated relationships among gut microbiota, metabolic function, and inflammation in adolescents with obesity at risk for type 2 diabetes (T2D).
- The aim of this study was to examine whether adolescents with obesity display variations in the microbiota associated with systemic inflammation or metabolic dysfunction.
- Variation in intestinal bacterial biomass, along with taxonomic composition, were associated with plasma lipids and insulin response among adolescents with obesity, with a greater impact on males.
- Variation in the intestinal microbiota is associated with metabolic and inflammatory dysregulation before T2D. Future sex-stratified studies through puberty are needed to inform strategies to reduce T2D.

The global increase in childhood obesity and earlier onset of type 2 diabetes (T2D) are a critical public health concern (1,2). Childhood obesity is robustly associated with adulthood obesity, T2D, and other metabolic complications (3,4). Early presentation of T2D displays greater

[1]Genetics and Genome Biology, The Hospital for Sick Children, Toronto, Ontario, Canada
[2]Department of Medical Biophysics, University of Toronto, Toronto, Ontario, Canada
[3]Department of Immunology, University of Toronto, Toronto, Ontario, Canada
[4]Division of Endocrinology, The Hospital for Sick Children, Department of Paediatrics, University of Toronto, Toronto, Ontario, Canada
[5]Cell Biology, The Hospital for Sick Children, Toronto, Ontario, Canada
[6]Department of Molecular and Cellular Biology, University of Guelph, Guelph, Ontario, Canada

Corresponding author: Jayne S. Danska, jayne.danska@sickkids.ca

Received 1 October 2024 and accepted 19 February 2025

This article contains supplementary material online at https://doi.org/10.2337/figshare.28444532.

A.G. and Q.Y.X. contributed equally to this work.

phenotypic heterogeneity and accelerated disease course in young patients (4), while return to a nonobese state before puberty reverses heightened risk of metabolic dysregulation in adulthood (3). These observations emphasize the need to investigate mechanisms of metabolic dysfunction in youth with obesity and for early intervention to delay or prevent progression to T2D and further metabolic complications.

A causal role of gut microbiota in the development of obesity has been demonstrated in mouse studies in which obese and lean phenotypes of adult human fecal donors have been transferred to recipient mice (5). In adult humans, obesity and metabolic dysfunction have been associated with gut microbiome composition, and functional capacity changes (6,7) most consistently decreased microbiome richness (8–10). However, most microbiome studies reported relative abundance composition analyses, which do not capture potential effects of variation in bacterial biomass. In inflammatory conditions, reduction in absolute bacterial biomass has been associated with decreased microbiome richness, increased abundance of certain bacterial taxa, and heightened proinflammatory responses (11–13). It is unknown whether perturbations in absolute bacterial biomass are present in adolescent obesity or metabolic dysfunction. Moreover, most studies compared individuals with obesity or metabolic disease with lean control individuals, overlooking the heterogeneity in progression to metabolic dysregulation in individuals with obesity. Our objective was to investigate relationships among the gut microbiota, metabolic dysfunction, and inflammation in youth with obesity to understand how these conditions originate and contribute to metabolic dysfunction.

Here, we characterized a cohort of adolescents enrolled in an obesity management program using high-throughput fecal 16S rRNA gene sequencing with absolute bacterial quantitation, high parameter single-cell analysis of peripheral blood mononuclear cells (PBMCs), and soluble inflammatory mediator quantification coanalyzed with clinical cardiometabolic measures. Among these participants, we observed multi–log differences in absolute fecal bacterial biomass that were associated with bacterial taxonomic composition. We identified sex-dependent associations among bacterial biomass, metabolic measures, and markers of systemic inflammation. Together, these results suggest that intestinal bacterial biomass and composition are associated with metabolic and inflammatory dysregulation in these youth at risk for metabolic disorders such as T2D and identify sex-specific regulation of metabolic dysfunction in adolescents with obesity.

RESEARCH DESIGN AND METHODS

Participant Recruitment

We evaluated a cohort of 56 adolescents from the Mechanisms of Inflammation, Immunity, Islet Cell and Intestinal Hormone Changes in Youth at Risk for Diabetes study aged 12–18 years with higher than the 97th percentile of age- and sex-standardized BMI based on the World Health Organization growth chart reference data for 5- to 19-year-olds (14). Adolescents provided stool samples at the time of their enrollment in the Healthy Living Program obesity management program at The Hospital for Sick Children (15). Study inclusion criteria included a stable BMI and no change in bowel movements for >3 months prior to recruitment. The recruited participants displayed no significant change in age- and sex-standardized BMI *z* score ($P = 0.59$ by paired *t* test) up to 6 months before the biospecimen collections for the current study. Exclusion criteria included a diagnosis of T2D or impaired glucose tolerance, taking medications known to alter glucose homeostasis (e.g., glucocorticoids, atypical antipsychotics), taking either probiotics or antibiotics <3 months before recruitment, or intercurrent illness, including mild infections, at the time of study entry. Participant demographic information is provided in Supplementary Table 1, and blood marker measurements are shown in Table 1. Additional assessment details are provided in the Supplementary Materials. This study was approved by the Research Ethics Board at The Hospital for Sick Children Healthy Living Clinic (IRB # 1000055159).

Stool Analysis

Stool genomic DNA was extracted using the QIAamp Fast DNA Stool Mini Kit (QIAGEN, Toronto, ON, Canada), and 16S rRNA gene sequencing was performed at the University of Colorado Anschutz Medical Campus. Host-free fecal bacterial culture in a continuous-flow bioreactor was performed as previously described (16,17). Absolute bacterial biomass was quantified using a Cell Viability Kit on an LSRFortessa Cell Analyzer (BD Biosciences). Detailed protocols are provided in the Supplementary Materials.

Immunophenotyping

A 34-marker cytometric time-of-flight (CyTOF) panel was designed for analyzing frozen viable PBMCs at the SickKids Centre for Advanced Single Cell Analysis with in-house–conjugated antibodies. The PBMC samples selected for the analysis represented the 1st and 4th quartiles of fecal bacterial biomass, with balanced sex in each biomass group and $>4 \times 10^6$ cells before freezing. Data transformation, quality control, gating, and Uniform Manifold Approximation and Projection (UMAP) were completed using CytoBank (Beckman Coulter Life Sciences). Detailed protocols, panel, and reagents are described in the Supplementary Material.

Statistical Analysis

For two-group comparisons, permutation test was used. Associations between continuous variables were performed using (generalized) linear regression. All statistical analyses were completed using R and corrected for multiple testing. The detailed statistical analysis is described in the Supplementary Material.

Table 1—Anthropometric and cardiometabolic measurements of participants

	Participants			
	Total (N = 56)	Male (n = 29)	Female (n = 27)	P
Anthropometric measurements				
Age (years)	56	15 (12–17)	16 (12–18)	0.74
Tanner stage	42			0.02
II–III	15	11	4	
IV–V	27	9	18	
Weight (kg)	56	114.0 (82.5–210.3)	105.6 (64.9–165.9)	0.19
BMI (kg/m^2)	56	38.7 (28.2–68.3)	40.6 (25.8–63.9)	0.74
Waist circumference (cm)	53	117.7 (99.1–176.5)	119.3 (90.2–161.5)	>0.99
Metabolic variables				
Fasting glucose (mmol/L)	56	4.8 (4.2–6.0)	4.8 (3.3–5.5)	0.39
Fasting insulin (μIU/mL)	56	26.1 (4.3–59.2)	17.56 (0.2–116.2)	0.12
ISI	38	4.2 (0.0–9.8)	2.8 (1.4–14.1)	0.29
HOMA-IR (glucose [mmol] × insulin [μIU/mL] / 22.5)	56	5.8 (0.9–15.8)	4.1 (1.4–9.2)	0.08
WBISI	41	1.6 (0.8–5.3)	2.1 (0.4–6.4)	0.19
HbA_{1c} (%)	53	5.2 (4.6–5.8)	5.3 (4.8–5.8)	0.42
CRP (mg/L)	46	3.1 (0.8–21.2)	5.7 (0.2–27.9)	0.14
Plasma lipids				
Cholesterol (mmol/L)	56	4.1 (2.8–6.4)	4.2 (2.2–6.5)	0.66
Triglycerides (mmol/L)	56	1.2 (0.7–2.8)	1.2 (0.5–2.9)	0.61
LDL (mmol/L)	56	2.6 (1.8–3.6)	2.4 (1.2–6.1)	0.53
HDL (mmol/L)	56	1.05 (0.5–1.9)	1.2 (0.6–1.8)	0.08

Data are n or median (range).

Data and Resource Availability

Original code is deposited at Github (https://github.com/quin97/MI4D). The 16S rRNA gene sequencing data are deposited at the National Center for Biotechnology Information under BioProject accession no. PRJNA1160259. Further information and requests should be directed to and will be fulfilled by the corresponding author.

RESULTS

Variation in Fecal Bacterial Biomass of Gut Bacteria in Adolescents With Obesity

To identify markers of progression to metabolic dysfunction, we studied a cohort of 56 adolescents with severe obesity (median BMI 39 kg/m^2) with normal glucose tolerance (Table 1). Age, sex, BMI, HOMA of insulin resistance (HOMA-IR), triglycerides, and self-reported race and ethnicity of the participants are provided in Supplementary Table 1.

To evaluate the gut microbiome in this cohort, we performed 16S rRNA gene sequencing on fecal-extracted genomic DNA. Gut microbiome composition based on relative abundance was comparable across most participants at the phylum level (Fig. 1*A*). To transform relative into absolute abundance, we enumerated bacteria from aliquots of the same fecal samples by flow cytometry and calibrated cell counts by dry stool weight given the varied stool water content due to diarrhea common in obesity (18). Across participant samples, we identified a multi–log variation of 3.8×10^9 to 5.5×10^{11} bacteria per gram of dry stool (Fig. 1*B*) associated with stool consistency (P = 0.003) (Supplementary Fig. 1*A*), suggesting that rapid intestinal transit time is negatively associated with absolute bacterial biomass (19). Previously, gut microbiome richness was reported to be decreased in adults with metabolic dysfunction and obesity compared with control individuals with normal weight (8–10). In this cohort, three measures of richness, including Chao1 index ($P = 8.45 \times 10^{-5}$) (Fig. 1*C*), Shannon index (P = 0.0008) (Supplementary Fig. 1*B*), and number of unique amplicon sequence variants (ASVs) (P = 0.0001) (Fig. 1*D*), were associated with fecal bacterial biomass.

Given these observations, we asked whether biomass was an intrinsic property of these gut microbiota by culturing fecal-derived bacterial communities in a host-free system. We used a nested case-control design, selecting fecal samples of participants from both the low and high biomass subgroups based on the median measure of 5.9×10^{10} bacteria per gram of dry stool (Fig. 1*E*). Gut bacterial communities of four participants from each of the two subgroups were cultured in a continuous flow, microprocessor-controlled bioreactor that modeled anaerobic conditions of the human distal colon, taking into consideration pH, nutrients, and flow rate (16,17). After stabilization over the first 5 days of culture, bioreactor cultures inoculated from participant high-biomass fecal samples displayed greater richness over time compared with cultures inoculated from participant low-biomass fecal samples ($P < 0.001$) (Fig. 1*F*), suggesting that gut bacterial communities retained features of taxonomic

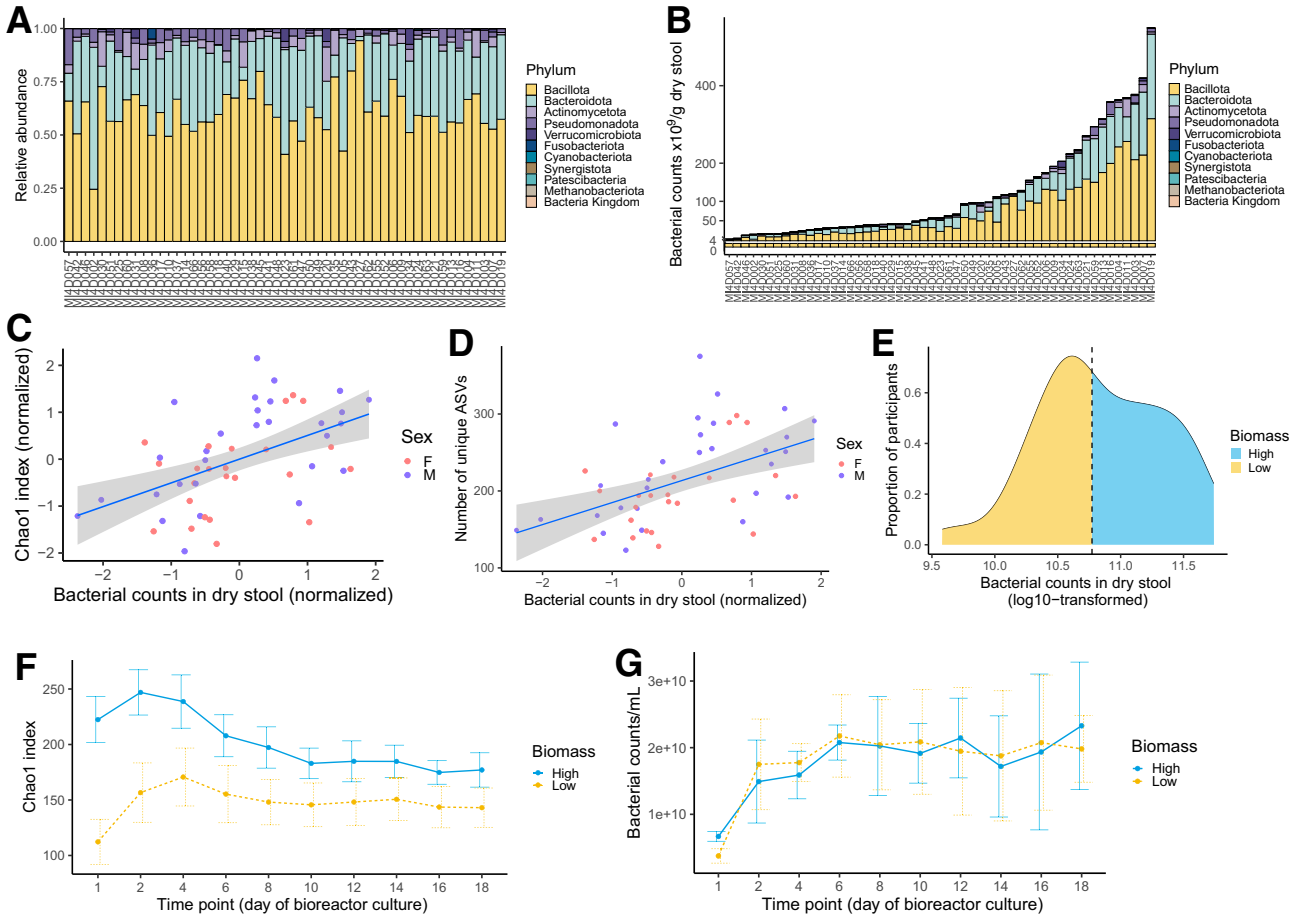

Figure 1—Gut microbiome profiling of adolescents with obesity. *A*: Bar plot of relative abundance of gut microbiome composition at the phylum level. *B*: Bar plot of absolute abundance of gut microbiome composition, scaled by bacterial counts in dry stool, at the phylum level. Fecal samples are in the same order of lowest to highest fecal bacterial biomass in *A*. *C*: Association between α-diversity (Chao1) and fecal bacterial biomass ($P = 8.45 \times 10^{-5}$). *D*: Association between the number of unique ASVs and fecal bacterial biomass in each sample ($P = 0.0001$). Associations were corrected for participant age, BMI, and sex. Normalization of continuous variables in stool was completed using caret version 6.0-85 based on center, scale, and Yeo-Johnson transformation. *E*: Participants were divided into low- and high-biomass groups based on the median of 5.9×10^{10} bacteria per gram of dry stool (range 3.8×10^{9} to 5.5×10^{11}). *F*: α-Diversity measurements in bioreactor-cultured communities derived from fecal samples from eight participants. α-Diversity of the cultures stabilized by day 5. α-Diversity of these cultures differed between low- and high-biomass samples ($P < 0.001$). *G*: Bacterial counts of bioreactor-cultured communities. The number of bacteria in the chemostat culture also stabilized after day 5. No significant differences were observed in the number of cultured bacteria between biomass groups ($P = 0.9$). Linear mixed models were used for testing differential Chao1 index and bacterial count across time points and biomass groups in the bioreactor culture. coeff, coefficient; F, female; M, male.

composition (Supplementary Fig. 1*C*) and richness (Chao1 index) (Fig. 1*F*) in a host-free system. In contrast, the difference in bacterial biomass observed in the source fecal samples was not sustained in these bioreactor cultures ($P = 0.9$) (Fig. 1*G*). Thus, while a robust association with gut microbiome richness was sustained in chemostat culture, fecal bacterial biomass behaved as a distinct feature of the community subject to host influences.

Gut Microbiome Composition Is Associated With Biomass and Sex

Within this cohort, 2,749 ASVs were identified, with mean relative abundance ranging from 0 to 3.5% (Supplementary Fig. 2*A* and *B*). Given the limited resolution of taxa and the sample size, we restricted the analysis to a core microbiome of 199 ASVs based on the inclusion criteria of ≥10% prevalence and ≥0.05% (1st quartile) mean relative abundance (Supplementary Fig. 2*A*). To identify factors contributing to variation in gut microbiome composition, we calculated Bray-Curtis dissimilarity as a measure of the community's β-diversity and plotted individual samples on projections that maximally correlated with participant characteristics using a distance-based redundancy analysis (dbRDA). Fecal bacterial count ($R^2 = 3.5\%$, $P = 0.0007$) (Fig. 2*A* and *B*) and participant sex ($R^2 = 3.4\%$, $P = 0.001$) (Fig. 2*C* and *D*) were the top two variables explaining a significant and non-redundant fraction of variation in microbiome composition followed by participant age ($R^2 = 3.0\%$, $P = 0.009$). The

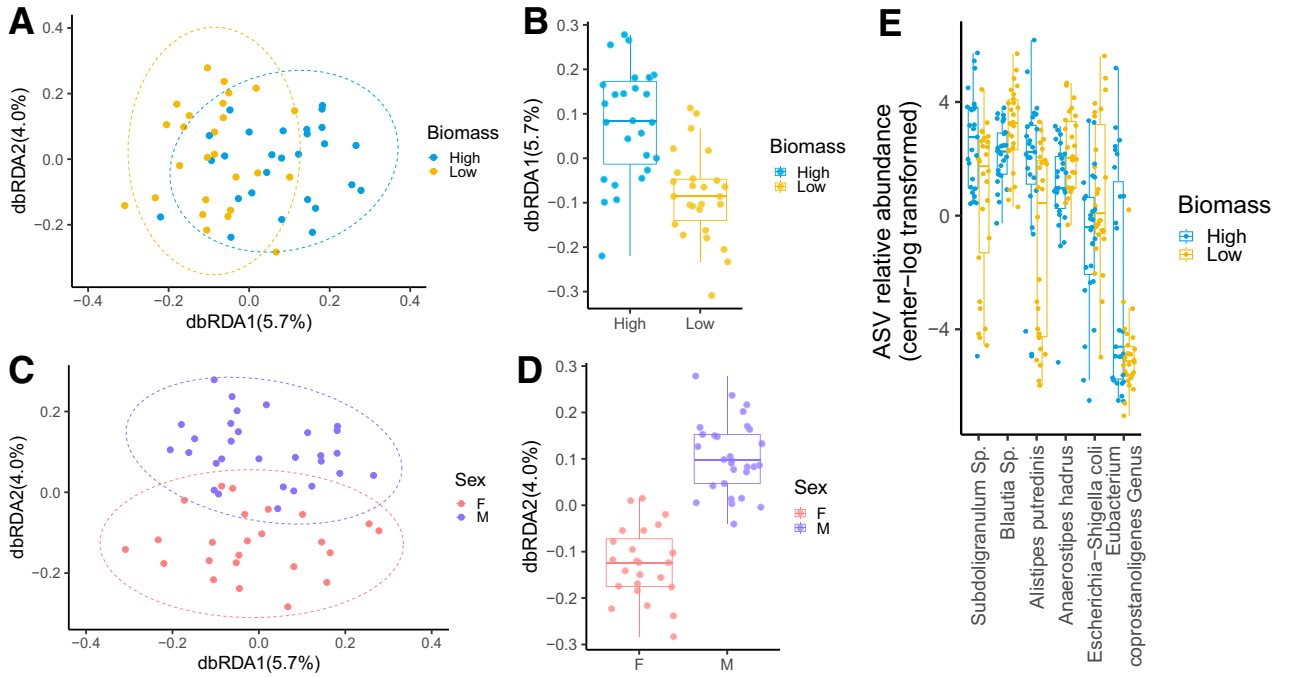

Figure 2—Association of gut bacterial composition with bacterial counts and participant sex. *A*: Projection of Bray-Curtis distance based on core microbiome relative abundance from 16S rRNA gene sequencing data onto the first two axes maximally correlated with age (R^2 = 2.9%, P = 0.009), sex (R^2 = 3.4%, P = 0.001), BMI (R^2 = 1.7%, P = 0.61), absolute bacterial count (R^2 = 3.5%, P = 0.0007), and fecal calprotectin levels (R^2 = 2.8%, P = 0.02) displayed with a dbRDA. Samples are colored by fecal bacterial biomass group. Ellipses represent 95% CIs for the estimated t distribution for each group. *B*: The dbRDA axis 1 coordinates for each sample of the high- and low-biomass groups. *C*: Projection of samples onto the first two dbRDA axes, colored by sex. Ellipses represent 95% CIs for the estimated t distribution for each group. *D*: Boxplot of dbRDA axis 2 coordinates for each sample separated by sex. *E*: Boxplot of the abundance of ASV relative abundance that displayed significant differences (adjusted P [p adj] < 0.1) between the low- and high-biomass groups from the top 20 ASVs contributing to dbRDA axis 1 (Supplementary Fig. 2*C*). Permutation tests were used to compare differential ASV relative abundance between the two groups and adjusted for multiple testing. F, female; M, male.

observed sex differences in gut microbiome composition were consistent with prior studies (20). The difference between the low- and high-biomass groups was most evident when the gut microbiome data were projected on dbRDA axis 1 (Fig. 2*A* and *B*). We identified differentially abundant ASVs between participants with low and high biomass from the top 20 ASVs contributing to this axis: *E. coli*, *Anaerostipes hadrus*, and *Blautia* species (sp.) were enriched in low-biomass gut microbiota; *Alistipes putredinis*, a *Subdoligranulum* sp., and *Eubacterium coprostanoligenes* were enriched in high-biomass gut microbiota (Fig. 2*E* and Supplementary Fig. 2*C*). Previously, individuals with a higher abundance of *Subdoligranulum variabile* achieved better insulin sensitivity in a fecal microbiota transplant trial (21). Moreover, the T2D microbiome has been shown to be enriched in *E. coli* and depleted in *Alistipes* and *Eubacterium* spp. (22). We also tested for differentially abundant ASVs between males and females from the top 20 ASVs contributing to dbRDA axis 2. An *Agathobacter* sp. was found to be enriched in males compared with females after multiple testing correction (Supplementary Fig. 2*D*). Collectively, these results suggest that gut microbiome composition differed between participants from the low- and high-biomass groups, with the latter harboring gut bacteria associated with benefits to host.

Metabolic Dysfunction Displays Sex-Specific Association With Bacterial Biomass and Composition

Unsupervised hierarchical clustering can be used to extract features based on interindividual variation and to enable stratification of individuals with dissimilar phenotypes in association with related metadata. This approach was previously used to evaluate associations among steady-state plasma glucose, multiomic measurements, and clinical metadata in adults with prediabetes (23). Here, we used hierarchical clustering for microbiome features of 199 core ASVs (Supplementary Fig. 3*A*) aggregated into 70 genera (Fig. 3*A*). The results identified three microbiome clusters. Cluster 1 membership decreased with increased microbial biomass (P = 0.007) (Fig. 3*B*), while cluster 2 membership increased with microbial biomass, corresponding to projection on dbRDA axis 1 (P = 0.02) (Fig. 3*B* and Supplementary Fig. 3*B*). Female participants were more often assigned to cluster 3, while male participants were more often assigned to clusters 1 and 2 (Supplementary Fig. 3*B*). Since this adolescent cohort had a similar number of males (n = 29) and females (n = 27), the differential frequency of male and female assignment into these clusters demonstrated sex differences in cluster membership. This result suggested that biomass and sex were two major drivers of variation in the gut

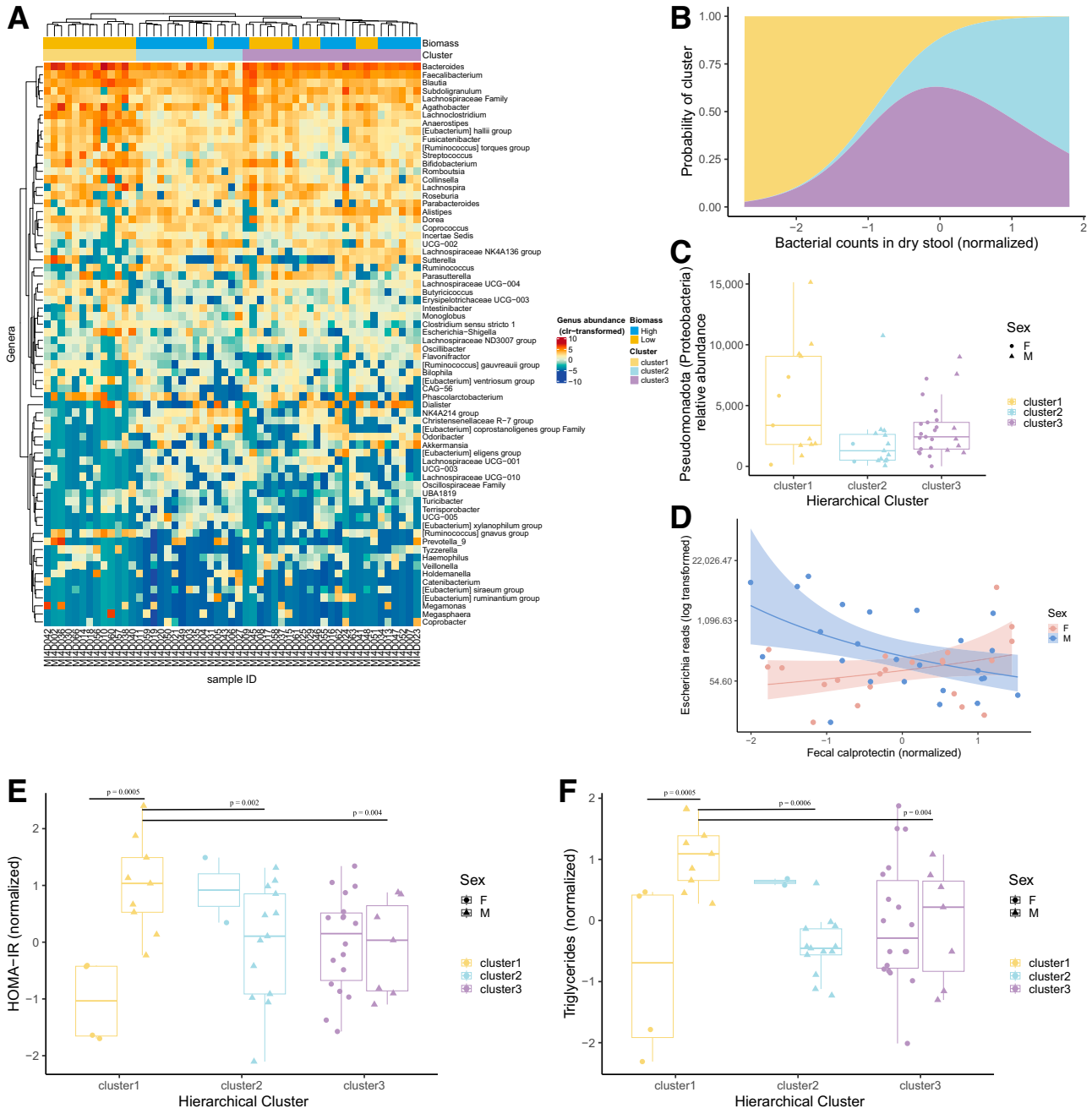

Figure 3—Fecal bacterial biomass is associated with microbiome composition and host metabolism. *A*: Heat map of core microbiome relative abundance at the genus level (n = 68) for all participants. Rows and columns are arranged by hierarchical clustering of Euclidean distance. Bacterial genera are aggregated based on ASVs used in dbRDA (ASV-level clustering in Supplementary Fig. 3*A*). Bacterial reads were center log-ratio (clr) transformed. *B*: Area plot of the probability of cluster assignment based on normalized fecal bacterial counts (multinomial logistic regression odds ratio 0.14, P = 0.007 for cluster 1; odds ratio 2.79, P = 0.02 for cluster 2). *C*: Pseudomonadota (Proteobacteria) relative abundance in the three main clusters. Relative abundance of Pseudomonadota differed across the three clusters (one-way ANOVA P = 0.022; post hoc Tukey honest significant difference adjusted P = 0.019 for cluster 2 vs. cluster 1, P = 0.096 for cluster 3 vs. cluster 1, P = 0.56 for cluster 3 vs. cluster 2). *D*: Association between *Escherichia*(*-Shigella*) genus abundance and fecal calprotectin (Gamma-generalized linear regression with log-link function P = 0.008 for sex, 0.03 for fecal calprotectin, and 9.4 $\times$ 10^{-6} for fecal calprotectin-sex interaction). *E*: Boxplot of normalized HOMA-IR values of participants stratified by cluster and sex (linear regression P = 0.0005 for sex, 0.002 for sex-cluster 2 interaction, and 0.004 for sex-cluster 3 interaction). *F*: Boxplot of normalized plasma triglyceride levels of participants stratified by cluster and sex (linear regression P = 0.0005 for sex, 0.0006 for sex-cluster 2 interaction, and 0.004 for sex-cluster 3 interaction). Normalization of HOMA-IR and triglycerides was completed using caret version 6.0-85 based on center, scale, and Yeo-Johnson transformation. Associations were corrected for participant age, BMI, and sex. F, female; ID, identifier; M, male.

microbiome of these participants corresponding to previous dbRDA findings (Fig. 2*A–D*). The composition of the three clusters differed at the phylum level, with higher relative abundance of Pseudomonadota (previously called Proteobacteria) in cluster 1 ($P = 0.022$) (Fig. 3*C*). After multiple testing adjustment, among highly prevalent (>75%) genera, the relative abundance of *Alistipes* ($P = 4.92 \times 10^{-4}$ for cluster 2, $P = 3.13 \times 10^{-5}$ for cluster 3), *Coprococcus* ($P = 0.014$ for cluster 3), *Lachnospiraceae NK4A136* group ($P = 0.015$ for cluster 3), and *UCG-002* ($P = 3.07 \times 10^{-6}$ for cluster 2, $P = 4.09 \times 10^{-5}$ for cluster 3) were significantly lower in cluster 1. *Escherichia* ($P = 0.035$ for cluster 2) and *Lachnoclostridium* ($P = 1.16 \times 10^{-4}$ for cluster 2) were significantly enriched in cluster 1 (Supplementary Fig. 3*D*). Among genera with <75% prevalence, a genus under *E. coprostanoligenes* group ($P = 3.46 \times 10^{-4}$), *Christensenellaceae R-7* group ($P = 0.017$), *NK4A214* group ($P = 0.018$), and *UCG-005* ($P = 1.07 \times 10^{-4}$) were each differentially distributed across clusters (Supplementary Fig. 3*E*).

Prior studies reported that Pseudomonadota retained a constant density despite reduced microbiota richness under inflammatory conditions (9,12). Indeed, we found that the absolute abundance of Pseudomonadota was not significantly different across clusters ($P = 0.078$) (Supplementary Fig. 3*C*), and no significant differences were found in *Escherichia*, the most prevalent genus of this phylum ($P = 0.365$). Some *Escherichia* strains can behave as pathobionts by crossing the gut barrier (24) and are correlated with calprotectin levels in patients with autoinflammatory conditions (11). To understand whether overrepresentation of *Escherichia* was similarly associated with inflammation in this cohort of adolescents with obesity, we quantified fecal and plasma calprotectin as markers of intestinal and systemic inflammation (25), respectively. No correlation was found between fecal and plasma levels of this protein (Supplementary Fig. 3*F*). Of note, the direction of association between *Escherichia* and fecal calprotectin differed between sexes. In female participants, fecal calprotectin level was positively associated with *Escherichia* relative abundance ($P = 0.03$) (Fig. 3*D*), whereas in males, the association was negative ($P = 9.4 \times 10^{-6}$) (Fig. 3*D*). After accounting for associations with sex and fecal calprotectin, *Escherichia* genus relative abundance was positively associated plasma calprotectin ($P = 0.01$) (Supplementary Fig. 3*G*). Given reports of Pseudomonadota-enriched gut bacteria in adults with obesity (6), we investigated whether microbiome clusters distinguished individuals with respect to their metabolic functions (Table 1). Measures of pancreatic β-cell function were derived from fasting insulin and fasting glucose (26–28), and HOMA-IR, whole-body insulin sensitivity index (WBISI), and insulinogenic index (IGI) were intercorrelated as expected (Supplementary Fig. 3*H*). Similarly, fasting blood lipids, total cholesterol level, HDL, LDL, and triglycerides were intercorrelated (Supplementary Fig. 3*I*). HOMA-IR and triglycerides were associated with microbiome clusters in a sex-specific manner in which the associations between lower biomass cluster and metabolic dysfunction were evident only in males (Fig. 3*E* and *F*). In cluster 1, composed of individuals having the lowest bacterial biomass, males displayed significantly higher insulin resistance based on HOMA-IR (Fig. 3*E*) compared with females ($P = 0.0005$). Males in cluster 2 and cluster 3, with higher bacterial biomass, had lower HOMA-IR levels compared with cluster 1 males ($P = 0.002$ and $P = 0.004$, respectively). Similarly, fasting triglyceride levels were highest among cluster 1 males compared with females ($P = 0.0005$), as well as higher in cluster 2 ($P = 0.0007$) and cluster 3 ($P = 0.004$) males. Note that sex differences were not significant in HOMA-IR or triglycerides when aggregated across clusters. The sex effect was only revealed by the association between microbiome clusters and metabolic measures (Table 1). Collectively, these results suggest that male adolescents with obesity and lower bacterial biomass, enriched in Pseudomonadota, manifested greater metabolic dysfunction measured by insulin resistance and fasting triglycerides.

Immune Profiles of Adolescents With Obesity Reveal Association With Fecal Bacterial Biomass

In adults with obesity, inflammation impacts multiple insulin responsive tissues that affect metabolic function and insulin action (29–34). Among immune cell populations, increased neutrophil and granulocytic myeloid-derived suppressor cell (G-MDSC) frequencies have been reported in participants with obesity and metabolic dysfunction (35–37). G-MDSCs, a heterogeneous population of low-density and neutrophil-like cells, confer immunosuppressive activity through production of calprotectin and other stress-inducing molecules (38). G-MDSCs likely represent neutrophils activated by exposure to cytokines during chronic inflammation, such as cancer and obesity (38). A high-fat diet can also promote differentiation of G-MDSCs by gut microbiota-derived metabolites (39), and adipose tissue inflammation can bias myeloid progenitors to generate proinflammatory neutrophil populations in settings of obesity (32).

Given that both microbiome analyses and metabolic measures from this adolescent cohort pointed toward underlying inflammation, we performed CyTOF immune profiling of 34 cell surface markers on PBMCs from participants in the low- and high-biomass groups ($n = 5$ per group) to evaluate potential differences across lymphoid and myeloid cell lineages. In the low-biomass group, we observed higher frequencies of $CD45^{lo}CD66b^{+}$ cells ($P = 0.04$) (Fig. 4*A* and *B*). In contrast to $CD14^{+}$ or $CD16^{+}$ peripheral blood monocytes (Supplementary Fig. 4*A*), these cells are $CD14^{lo}CD16^{hi}$and express low levels of HLA-DR, CD11b, and CD11c, corresponding to surface phenotypes of low-density neutrophils, including G-MDSCs, which were retained in the PBMC fraction after gradient centrifugation.

We compared frequencies of major leukocyte populations, T-cell receptor (TCR) αβ-cells, TCRγδ-cells, B cells, natural killer (NK) cells/innate lymphoid cells (ILCs), and myeloid cells among these study participants, and did not observe

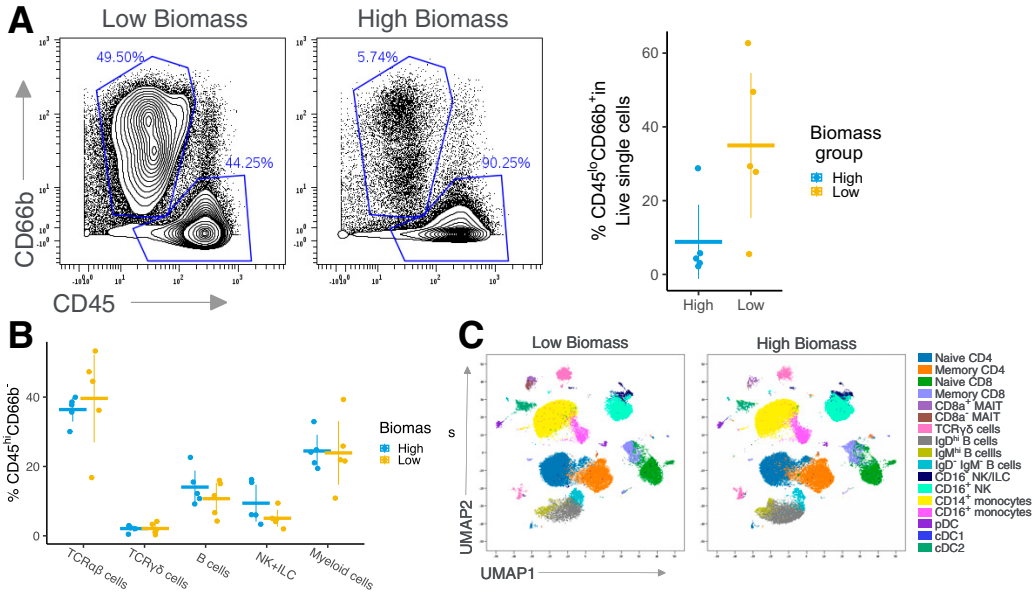

Figure 4—CyTOF immune profiling of PBMCs from participants in the low and high fecal bacterial biomass groups. PBMCs were stained with a panel of metal-tagged antibodies to immune cell markers and analyzed by CyTOF. Data were preprocessed as described in the Supplementary Material. *A*: Left, contour plots (5% probability) show CD66b vs. CD45 expression in live single cells from exemplars of each biomass group, showing gates (blue polygons) used to quantify $CD45^{lo}CD66b^{+}$ low-density neutrophils and $CD45^{hi}CD66b^{-}$ cells. Right, frequencies of $CD45^{lo}CD66b^{+}$ low-density neutrophils among live single PBMCs in each biomass group ($P = 0.04$, permutation test). *B*: Frequencies of major immune cell subsets in the $CD45^{hi}CD66b^{-}$ population from each group. Horizontal lines depict the mean in each group, with error bars representing 2 SDs from the mean. T cells (TCRαβ and TCRγδ subsets), B cells, NK cells + ILCs, and myeloid cells were gated based on CD3, TCRγδ, CD19, HLA-DR, and CD7. The gating hierarchy is described in the Research Design and Methods. No differentially abundant cell subsets were found ($P > 0.05$ for all cell subsets, permutation test). *C*: UMAP dimensionality reduction of the $CD45^{hi}CD66b^{-}$ population were overlaid with the indicated manually gated populations quantified in *B* and Supplementary Fig. 4*B–D*. Exemplars of each biomass group are shown. cDC, conventional dendritic cell; ILC, innate lymphoid cell; MAIT, mucosal-associated invariant T cell; NK, natural killer cell; pDC, plasmacytoid dendritic cell.

significant differences between the low- and high-biomass groups (Fig. 4*B*). Frequencies of T cell, B cell, and myeloid cell subsets were comparable between the low- and high-biomass groups (Supplementary Fig. 4*B–D*). Visualization of these subsets on unsupervised UMAP of the $CD45^{hi}CD66b^{-}$ population showed that our manual gating strategy captured most cells and did not reveal associations with the high- or low-biomass group across the cohort (Fig. 4*C*). The most evident difference in immune profiles between the low- and high-biomass groups was the low-density neutrophils (Fig. 4*A*). However, PBMC preparations did not allow reliable neutrophil enumeration.

To follow up on a potential difference in neutrophil frequencies between the low- and high-biomass groups, elastase (20,36), calprotectin (32,37), and myeloperoxidase (36) were quantified in plasma samples isolated at the time of PBMC preparation as measures of neutrophil activity. The three neutrophil-associated proteins were highly correlated (Supplementary Fig. 5*A*) and displayed sex-dependent associations with fecal bacterial biomass (Fig. 5*A–C*). Specifically, there was no association between fecal microbial biomass and neutrophil plasma proteins in female participants, while in male participants, we observed a significant negative association between bacterial biomass and neutrophil plasma proteins (for interaction with sex, elastase $P = 0.02$, calprotectin $P = 0.01$, myeloperoxidase $P = 0.03$). Since microbiome composition and fecal bacterial biomass were associated with metabolic measures (Fig. 3*E* and *F*), we asked whether plasma neutrophil-associated protein levels were similarly associated. Indeed, we identified positive associations between the three neutrophil-associated proteins and triglyceride levels across the entire cohort (Fig. 5*D–F*) (elastase $P = 0.02$, calprotectin $P = 0.02$, myeloperoxidase $P = 0.004$). These findings concur with prior reports suggesting neutrophil involvement in obesity and metabolic dysfunction (30,32,35–37). To evaluate whether the serum neutrophil and lipid markers observed in this cohort were associated with bacterial endotoxin translocation (40) into the circulation, we quantified plasma mediators binding to bacterial lipopolysaccharide (LPS), soluble CD14 (sCD14) and LPS-binding protein (LBP). LBP and sCD14 levels were correlated (Supplementary Fig. 5*A*) but were not associated with fecal bacterial biomass. LBP, however, was significantly associated with levels of the inflammatory marker C-reactive protein (CRP), suggesting that acute phase response proteins were not coordinated with neutrophil activities in this cohort with obesity ($P = 0.001$) (Supplementary Fig. 5*B*). Taken together, these results suggest that under conditions of low fecal microbial biomass, male adolescents with obesity demonstrate a greater degree

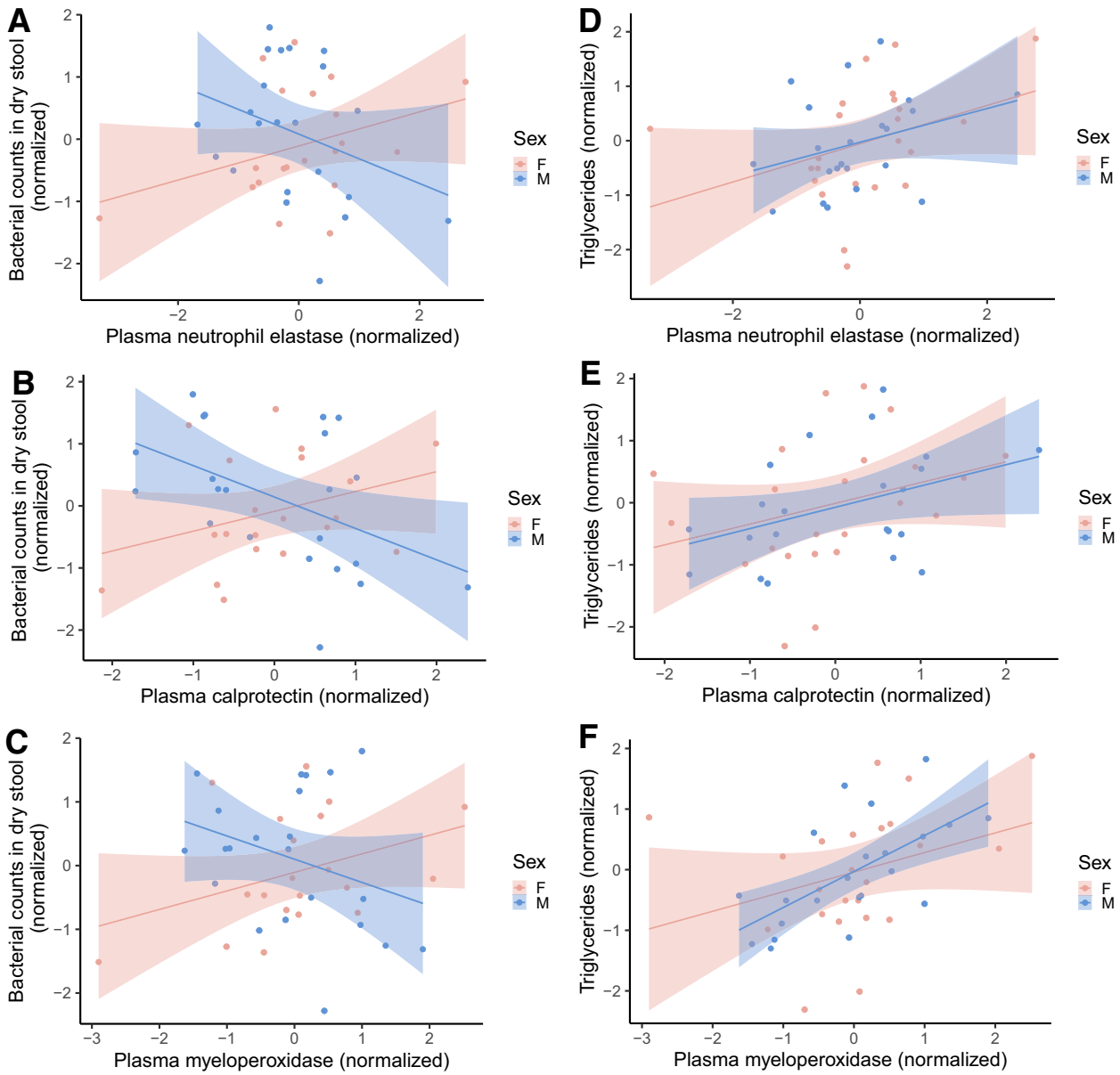

Figure 5—Sex-specific associations of plasma neutrophil elastase (ELA2) (interaction term $P = 0.02$) (*A*), calprotectin (interaction term $P = 0.01$) (*B*), and myeloperoxidase (MPO) (interaction term $P = 0.03$) (*C*) to fecal bacterial biomass are shown. Associations of plasma ELA2 ($P = 0.02$) (*D*), calprotectin ($P = 0.02$) (*E*), and MPO ($P = 0.004$) (*F*) to plasma triglycerides are also shown. Associations were tested by linear regression, color-coded by sex, and adjusted for age, sex, and BMI. Normalization of continuous variables was completed using caret version 6.0-85 based on center, scale, and Yeo-Johnson transformation. F, female; M, male.

of systemic inflammation and metabolic dysfunction compared with age-matched females.

Modeling Relationships Among Gut Microbes, Metabolism, and Inflammation

A previous study in adults demonstrated associations among gut microbiome composition, absolute bacterial load, adiposity, and markers of systemic inflammation that were modified by statin intake (10). To compare our results with previous findings, we used exploratory structural equation modeling (ESEM) to examine how alterations in gut microbiota and systemic inflammation might contribute to metabolic dysregulation. ESEM was used to estimate the relationships between these latent variables and contributions from observed variables (Fig. 6). The latter was modeled based on the source of biological samples (e.g., stool, plasma) and current understanding of biological pathways in these tissues. We modeled the gut microbiota (Fig. 6, blue circle) using microbiome clusters from Fig. 3*A*, fecal calprotectin, and stool consistency. The bacterial biomass was included as a distinct variable from gut microbiota to account for its host dependency (Fig. 1*F* and *G*). The observed variables that explained the greatest variance in gut microbiota were stool consistency,

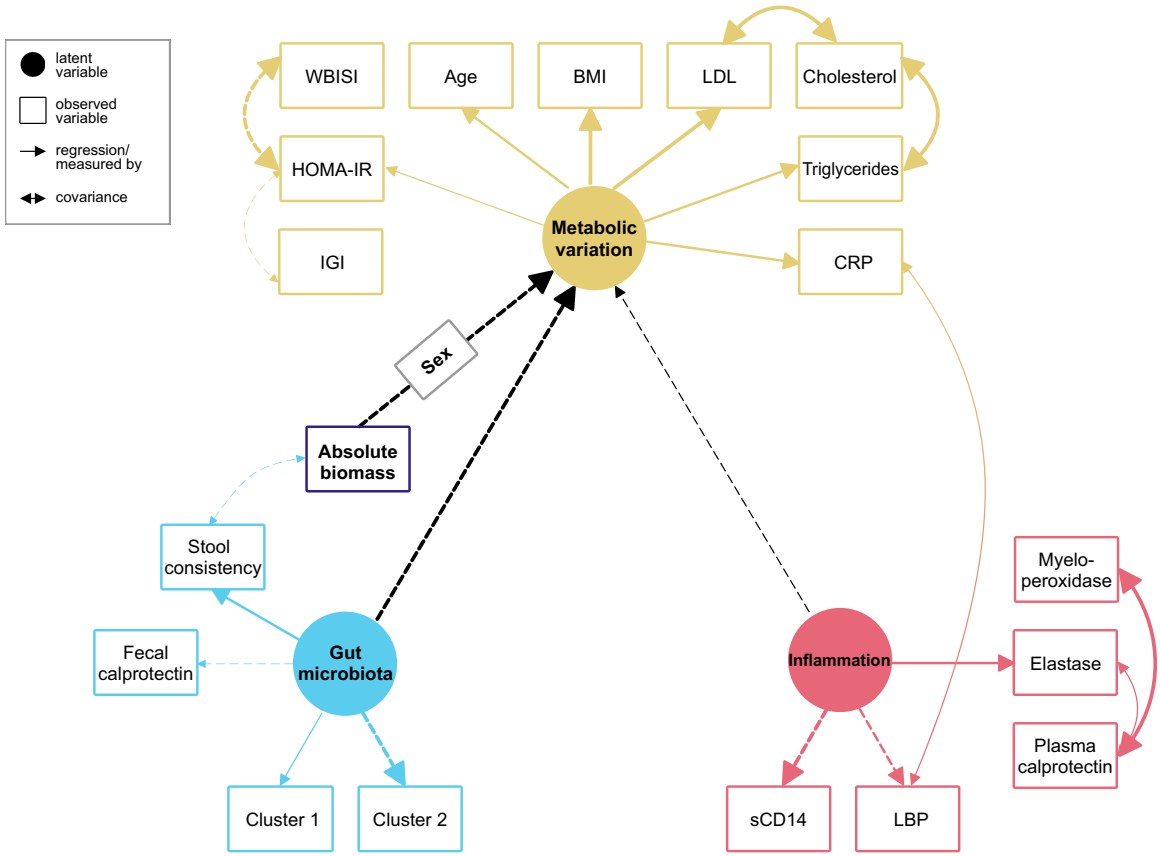

Figure 6—ESEM of the interactions among three latent variables summarizing variation in the gut microbiota, inflammation, and metabolic parameters. These latent variables (filled circles) are indicated by a set of observed variables (unfilled rectangles). The colored unidirectional arrows represent the contribution of observed variables toward latent variables. The black unidirectional arrows represent regression. Covariance between observed variables is represented by colored bidirectional arrows. All variables modeled, except for categorial variables (sex and cluster assignments), were normalized. Solid lines indicate positive associations, and dashed lines indicate negative associations. Line thickness corresponds to the robustness of the association estimated by the model indicated by *P* values (cutoff of 0.1 used for the model). Coefficients and statistics are provided in Supplementary Table 2.

followed by microbiome cluster 2, which was most prevalent in the higher biomass subgroup. These two variables contributed to the gut microbiota with opposite directions of effect, corresponding to a healthier phenotype with cluster 2 membership and lower stool water content. Variance in metabolism was modeled using plasma lipid levels, glycemic control, and CRP (Fig. 6, tan circle), which were estimated to comprise two factors contributing to metabolic variation, one of which consisted of blood lipids, triglycerides, and LDL (Supplementary Table 2). For both factors, adverse metabolic parameters were assigned positive coefficients, with higher HOMA-IR, LDL, and triglycerides reflecting insulin resistance and dyslipidemia. In accordance with clinical interpretation, higher IGI, which indicates better β-cell function, and WBISI, a measure of insulin sensitivity, were both estimated to have negative covariance with HOMA-IR (26,27). Measurements of inflammation included the three neutrophil-associated proteins with significant covariance and the two proteins involved in the endotoxin response (Fig. 6, red circle). For the latent variables, metabolic dysfunction was modeled to result from variation in gut microbiota, systemic inflammation, fecal bacterial biomass, and sex. Notably, the interaction between fecal bacterial biomass and sex displayed significant covariance with gut microbiota.

As we report here, previous studies in adults observed associations between dyslipidemia and measures of systemic inflammation, including neutrophil proteins, low-density neutrophil frequencies, and inflammatory cytokines such as interleukin 6, interleukin 1β, and tumor necrosis factor-α (10,23,35). We found an association between higher fecal microbial biomass with firmer stool consistency and greater bacterial diversity, as well as with reduced proportions of taxa associated with inflammatory properties and lower levels of serum markers of systemic inflammation. Similar relationships were reported in studies of adults (10,11,13). Moreover, we identified sex-dependent associations of gut microbiome features and fecal bacterial biomass with markers of metabolic dysfunction. Taken together, the model integrated a relationship between alterations in gut microbiota,

driven by stool consistency and biomass, and systemic inflammation contributing to metabolic dysfunction in the adolescent males of this cohort. Future studies need to account for these parameters to elucidate relationships among gut microbiota, inflammation, and sex in progression from obesity to metabolic dysfunction in adolescents.

DISCUSSION

Gut microbiota have been implicated in obesity and metabolic dysfunction. While changes in taxonomical composition and metabolites of the gut microbiota have been observed in obesity and T2D (5,6,10), most association studies were not designed to capture microbial biomass, indicative of a perturbed gut ecosystem under proinflammatory conditions (11–13). In this study, we measured the absolute and relative abundance of gut bacteria, along with immunometabolic profiling, in a cohort of adolescents with obesity. We observed multi–log differences in fecal bacterial biomass that were correlated with richness of the gut microbiome and stool consistency. Previously, both rapid transit time (17,18) and decreased richness of the gut microbiome (8–10) have been associated with obesity and metabolic dysfunction. In contrast to adult studies, we did not observe an association of BMI with microbiome composition (10,20) or changes in ratios between Bacillota (Firmicutes) and Bacteroidota (Bacteroidetes) reported in adults with obesity (5,41). The lack of association in our study could reflect differences in study population, the ranges of BMI, and the limitation in defining adolescent obesity using BMI (42), as well as the potential difference in underlying mechanisms of obesity in childhood and adulthood.

The top variable explaining variance in the gut microbiome in this cohort was fecal bacterial biomass. Among the taxa enriched in high biomass group, *A. putredinis* has been associated with the benefit of physical activity and improved metabolism in healthy adults, including less weight gain with age and lower plasma HbA_{1c} levels (43); *E. coprostanoligenes* has been shown to encode cholesterol dehydrogenases and has been associated with lower cholesterol levels (44). The butyrate producers *A. hadrus* and *Blautia* were enriched in the low-biomass group, whereas *Subdoligranulum* sp. was enriched in the high-biomass group (45). Intriguingly, while changes in relative abundance of *Blautia* has been implicated in multiple studies of metabolic dysfunction (23,46), others have demonstrated a beneficial effect on host metabolism (6,47). Among various evidence associating short-chain fatty acids (SCFAs) with obesity (5,7,19,41), increased SCFA-producing bacterial taxa have been observed in children with obesity (48) and hypothesized to confer energy for the host through lipid biosynthesis. We also observed enriched Pseudomonadota in participants in the low-biomass group, possibly attributed to its capability of sustaining constant density in a proinflammatory environment at the expense of other phyla (12). LPS and proinflammatory cytokines resulting from infection by pathogenic strains of *E. coli* can fuel innate immune responses and cause significant tissue damage in the gut (24). In mouse models, infection with a murine equivalence of pathogenic *E. coli* strain led to gut microbiome compositions enriched in phage and bacterial metabolic genes, driving short-term microbiota adaptation at the subspecies level (49). These studies demonstrated the connectedness between bacterial composition and biomass resulting from the interactions between bacterial metabolic pathways in the community. Additionally, we saw that the host differences in the α-diversity measures of gut microbiome composition were preserved in bioreactor cultures of gut bacterial communities. In contrast, host differences in fecal microbial biomass were no longer significant after culture. These findings suggest that fecal bacterial biomass is subject to influences of the host environment rather than reflecting an inherent property of the gut microbial community. A study of a patient with rapid-onset obesity with hypoventilation, hypothalamic, and autonomic dysregulation demonstrated increased fecal bacterial biomass and richness following bariatric surgery–induced weight loss (50). Additionally, gut composition (41) and fecal bacterial biomass can be modified through changes in diet (12,49). In mouse models, fat and starch-based diets can decrease the absolute abundance of bacteria in feces (49), and carnivorous diets are significantly associated with reduced gut microbial densities compared with noncarnivorous diets in mammals (12).

While metabolic inflammation has been attributed to increased myeloid cell infiltration in the adipose tissue (30,32,51), we did not observe significant differences in major PBMC populations between the low- and high-biomass groups. Similar results were observed in a small adult cohort in which the plasma cytokine levels were not different between individuals with metabolically healthy and unhealthy obesity (52). In contrast, we observed a higher frequency of low-density neutrophils in PBMCs from participants in the low-biomass group. Low-density neutrophils were found to be increased in patients with severe obesity and decreased following bariatric surgery–induced weight loss (35). We validated our CyTOF immunophenotype analysis by quantification of neutrophil-associated proteins in plasma and found an association of these proteins with fasting triglycerides and absolute bacterial biomass. Stratification of participants based on gut microbiome composition and fecal bacterial biomass revealed sex-specific associations with metabolic status and inflammation markers. In male adolescents with obesity, lower bacterial biomass was associated with greater metabolic dysregulation and elevated systemic inflammation attributed to neutrophil activities. Previous studies have investigated sex differences in associations between insulin resistance and other markers of metabolic dysfunction, including hepatic stenosis, branched-chain amino acid levels, and lipoprotein subclasses, in children and adolescents with obesity (53–55). For example, steatohepatitis was associated with insulin resistance and visceral fat in both sexes and in

males, with steroid hormone levels, body fat distribution, and markers of inflammation (53). In contrast, visceral adiposity, BMI *z* score, and branched-chain amino acid levels were found to be associated with abundances of lipoprotein subclasses only in females (55,55). The sex-specific associations we observed in the current study cohort may reflect differences in immune responses. Compared with males, neutrophils in healthy females displayed a higher expression of type I interferon–stimulated genes that were hormone-dependent (56). Our observations may also be explained by sex differences in fat deposition, energy expenditure, and tissue insulin sensitivity (57). In particular, the effects of testosterone display sex differences for which higher levels were associated with an elevated T2D risk in females but a lower risk in males (57). Such sex differences may contribute to the increased prevalence of metabolic health in females with obesity compared with males (52).

Our results suggest that intestinal bacterial biomass is associated with gut microbiome composition, stool consistency, and metabolic status in adolescents with obesity. Overall, individuals with high fecal biomass displayed healthier intestinal, metabolic, and inflammatory parameters, while lower bacterial biomass was associated with greater metabolic dysregulation and elevated systemic neutrophil activity in male adolescents with obesity. These observations highlight the importance of additional investigations of the role of biological sex in regulating metabolism and immune responses in adolescence.

Study Limitations

Our study examined a cross-sectional cohort of adolescents with obesity and without diabetes to identify risk factors for metabolic dysfunction. The cross-sectional design limited inference regarding causes of metabolic dysfunction in these adolescents and identification of potential confounders for the observed associations. A longitudinal study design would be required to determine whether perturbations in gut microbiota and higher neutrophil numbers or activity precede metabolic dysregulation. The cohort size was relatively small, limiting power to detect additional potentially significant differences in immune cell populations, as well as correlates of metabolic variation. The majority of the study participants self-identified as White. Recruitment of more diverse study participants will be needed for future studies to determine whether the current findings are generalizable to other ancestries, including equity-deserving groups who are significantly burdened by trends of youth-onset obesity. Puberty and diet are potentially important factors that impact metabolism and gut microbiota (58,59). However, we were not able to incorporate these variables into our analysis due to inconsistencies in self-reported dietary recall and missing data for self-reported Tanner stage. Despite these limitations, we identified robust sex differences in associations between bacterial biomass and metabolic measurements in adolescents with obesity that provide evidence for important relationships of gut microbiota with metabolic dysfunction and inflammation in youth.

Acknowledgments. The authors thank Steve Mortin-Toth (The Hospital for Sick Children) for help with PBMC processing and sample inventory, Lisa Chu and Shawna Steele (The Hospital for Sick Children) for grant writing and participant recruitment, Dr. Alexandra Paun (McGill University) for consultation on bioinformatics analyses, and Dr. Daniel N. Frank (University of Colorado) for high-throughput sequencing services.

Funding. A.G. was supported by the LiUNA! Fellowship for Research Innovation from the SickKids Restracomp program. This work was funded by operating grants from the Canadian Institutes of Health Research (CIHR J.S.D. and J.H.), Breakthrough T1D, formerly JDRF (J.S.D. and E.A.V.), the Anne and Max Tanenbaum Chair in Molecular Medicine, University of Toronto (J.S.D.), and the Hospital for Sick Children Research Institute (J.S.D.). Mass cytometry was performed at the SickKids Centre for Advanced Single Cell Analysis, supported by the SickKids Foundation and a Canadian Foundation for Innovation John Evans Fund Leaders grant (to C.J.G.).

Duality of Interest. No potential conflicts of interest relevant to this article were reported.

Author Contributions. A.G., Q.Y.X., E.A.-V., C.J.G., J.K.H., and J.S.D. contributed to the study conceptualization. A.G., Q.Y.X., A.W., C.Y., T.C., C.G.-H., E.A.-V., C.J.G., and J.S.D. contributed to the investigation. A.G., Q.Y.X., C.Y., R.N., T.C., C.G.-H., E.A.-V., C.J.G., and J.S.D. contributed to the methodology. Q.Y.X. and J.S.D. wrote the original draft of the manuscript. All authors reviewed and edited the manuscript. J.K.H. and J.S.D. acquired funding. J.K.H. and J.S.D. are the guarantors of this work and, as such, had full access to all the data in the study and take responsibility for the integrity of the data and the accuracy of the data analysis.

References

1. Abarca-Gómez L, Abdeen ZA, Hamid ZA, et al. Worldwide trends in body-mass index, underweight, overweight, and obesity from 1975 to 2016: a pooled analysis of 2416 population-based measurement studies in 128·9 million children, adolescents, and adults. Lancet 2017;390:2627–2642

2. Wagenknecht LE, Lawrence JM, Isom S, et al.; SEARCH for Diabetes in Youth study. Trends in incidence of youth-onset type 1 and type 2 diabetes in the USA, 2002–18: results from the population-based SEARCH for Diabetes in Youth study. Lancet Diabetes Endocrinol 2023;11:242–250

3. Bjerregaard LG, Jensen BW, Ängquist L, Osler M, Sørensen TIA, Baker JL. Change in overweight from childhood to early adulthood and risk of type 2 diabetes. N Engl J Med 2018;378:1302–1312

4. Misra S, Ke C, Srinivasan S, et al. Current insights and emerging trends in early-onset type 2 diabetes. Lancet Diabetes Endocrinol 2023;11:768–782

5. de Wit DF, Hanssen NMJ, Wortelboer K, Herrema H, Rampanelli E, Nieuwdorp M. Evidence for the contribution of the gut microbiome to obesity and its reversal. Sci Transl Med 2023;15:eadg2773

6. Baars DP, Fondevila MF, Meijnikman AS, Nieuwdorp M. The central role of the gut microbiota in the pathophysiology and management of type 2 diabetes. Cell Host Microbe 2024;32:1280–1300

7. Byndloss M, Devkota S, Duca F, et al. The gut microbiota and diabetes: research, translation, and clinical applications—2023 Diabetes, Diabetes Care, and Diabetologia Expert Forum. Diabetologia 2024;67:1760–1782

8. Cotillard A, Kennedy SP, Kong LC, et al.; ANR MicroObes Consortium. Dietary intervention impact on gut microbial gene richness. Nature 2013;500:585–588

9. Le Chatelier E, Nielsen T, Qin J, et al.; MetaHIT Consortium. Richness of human gut microbiome correlates with metabolic markers. Nature 2013;500:541–546

10. Vieira-Silva S, Falony G, Belda E, et al.; MetaCardis Consortium. Statin therapy is associated with lower prevalence of gut microbiota dysbiosis. Nature 2020;581:310–315
11. Vieira-Silva S, Sabino J, Valles-Colomer M, et al. Quantitative microbiome profiling disentangles inflammation- and bile duct obstruction-associated microbiota alterations across PSC/IBD diagnoses. Nat Microbiol 2019;4:1826–1831
12. Contijoch EJ, Britton GJ, Yang C, et al. Gut microbiota density influences host physiology and is shaped by host and microbial factors. Elife 2019;8:e40553
13. Vandeputte D, Kathagen G, D'hoe K, et al. Quantitative microbiome profiling links gut community variation to microbial load. Nature 2017;551:507–511
14. World Health Organization. BMI-for-age (5–19 years). Accessed 7 June 2024. Available from https://www.who.int/tools/growth-reference-data-for-5to19-years/indicators/bmi-for-age
15. Luca P, Dettmer E, Khoury M, et al. Adolescents with severe obesity: outcomes of participation in an intensive obesity management programme. Pediatric Obesity 2015;10:275–282
16. Gianetto-Hill CM, Vancuren SJ, Daisley B, et al. The robogut: a bioreactor model of the human colon for evaluation of gut microbial community ecology and function. Current Protocols 2023;3:e737
17. Granato A, Renwick S, Yau C, et al.; DIABIMMUNE Study Group. Analysis of early childhood intestinal microbial dynamics in a continuous-flow bioreactor. Microbiome 2024;12:255
18. Ballou S, Singh P, Rangan V, Iturrino J, Nee J, Lembo A. Obesity is associated with significantly increased risk for diarrhoea after controlling for demographic, dietary and medical factors: a cross-sectional analysis of the 2009-2010 National Health and Nutrition Examination Survey. Aliment Pharmacol Ther 2019;50:1019–1024
19. Müller M, Hermes GDA, Canfora EE, et al. Distal colonic transit is linked to gut microbiota diversity and microbial fermentation in humans with slow colonic transit. Am J Physiol Gastrointest Liver Physiol 2020;318:G361–G369
20. Rothschild D, Leviatan S, Hanemann A, Cohen Y, Weissbrod O, Segal E. An atlas of robust microbiome associations with phenotypic traits based on large-scale cohorts from two continents. PLoS One 2022;17:e0265756
21. Kootte RS, Levin E, Salojärvi J, et al. Improvement of insulin sensitivity after lean donor feces in metabolic syndrome is driven by baseline intestinal microbiota composition. Cell Metab 2017;26:611–619.e6
22. Mei Z, Wang F, Bhosle A, et al. Strain-specific gut microbial signatures in type 2 diabetes identified in a cross-cohort analysis of 8,117 metagenomes. Nat Med 2024;30:2265–2276
23. Zhou W, Sailani MR, Contrepois K, et al. Longitudinal multi-omics of host–microbe dynamics in prediabetes. Nature 2019;569:663–671
24. Fernandez MI, Sansonetti PJ. Shigella interaction with intestinal epithelial cells determines the innate immune response in shigellosis. Int J Med Microbiol 2003;293:55–67
25. Jukic A, Bakiri L, Wagner EF, Tilg H, Adolph TE. Calprotectin: from biomarker to biological function. Gut 2021;70:1978–1988
26. Retnakaran R, Qi Y, Goran MI, Hamilton JK. Evaluation of proposed oral disposition index measures in relation to the actual disposition index. Diabet Med 2009;26:1198–1203
27. Singh B, Saxena A. Surrogate markers of insulin resistance: A review. World J Diabetes 2010;1:36–47
28. de Cassia da Silva C, Zambon MP, Vasques ACJ, Camilo DF, Reis de Góes Monteiro Antonio MÂ, Geloneze B. The threshold value for identifying insulin resistance (HOMA-IR) in an admixed adolescent population: a hyperglycemic clamp validated study. Arch Endocrinol Metab 2023;67:119–125
29. Chavakis T, Alexaki VI, Ferrante AW. Macrophage function in adipose tissue homeostasis and metabolic inflammation. Nat Immunol 2023;24:757–766
30. Mansuy-Aubert V, Zhou QL, Xie X, et al. Imbalance between neutrophil elastase and its inhibitor α1-antitrypsin in obesity alters insulin sensitivity, inflammation, and energy expenditure. Cell Metab 2013;17:534–548
31. Muir LA, Cho KW, Geletka LM, et al. Human CD206+ macrophages associate with diabetes and adipose tissue lymphoid clusters. JCI Insight 2022;7:e146563
32. Nagareddy PR, Kraakman M, Masters SL, et al. Adipose tissue macrophages promote myelopoiesis and monocytosis in obesity. Cell Metab 2014;19:821–835
33. Hildreth AD, Ma F, Wong YY, Sun R, Pellegrini M, O'Sullivan TE. Single-cell sequencing of human white adipose tissue identifies new cell states in health and obesity. Nat Immunol 2021;22:639–653
34. Schleh MW, Caslin HL, Garcia JN, et al. Metaflammation in obesity and its therapeutic targeting. Sci Transl Med 2023;15:eadf9382
35. Sanchez-Pino MD, Richardson WS, Zabaleta J, et al. Increased inflammatory low-density neutrophils in severe obesity and effect of bariatric surgery: results from case-control and prospective cohort studies. eBioMedicine 2022;77:103910
36. Ali M, Jasmin S, Fariduddin M, Alam SMK, Arslan MI, Biswas SK. Neutrophil elastase and myeloperoxidase mRNA expression in overweight and obese subjects. Mol Biol Rep 2018;45:1245–1252
37. Nijhuis J, Rensen SS, Slaats Y, van Dielen FMH, Buurman WA, Greve JWM. Neutrophil activation in morbid obesity, chronic activation of acute inflammation. Obesity (Silver Spring) 2009;17:2014–2018
38. Veglia F, Sanseviero E, Gabrilovich DI. Myeloid-derived suppressor cells in the era of increasing myeloid cell diversity. Nat Rev Immunol 2021;21:485–498
39. Chen J, Liu X, Zou Y, et al. A high-fat diet promotes cancer progression by inducing gut microbiota–mediated leucine production and PMN-MDSC differentiation. Proc Natl Acad Sci USA 2024;121:e2306776121
40. Thaiss CA, Levy M, Grosheva I, et al. Hyperglycemia drives intestinal barrier dysfunction and risk for enteric infection. Science 2018;359:1376–1383
41. Van Hul M, Cani PD. The gut microbiota in obesity and weight management: microbes as friends or foe? Nat Rev Endocrinol 2023;19:258–271
42. Hadjiyannakis S, Ibrahim Q, Li J, et al. Obesity class versus the Edmonton Obesity Staging System for Pediatrics to define health risk in childhood obesity: results from the CANPWR cross-sectional study. Lancet Child Adolesc Health 2019;3:398–407
43. Wang K, Mehta RS, Ma W, et al. The gut microbiome modifies the associations of short- and long-term physical activity with body weight changes. Microbiome 2023;11:121
44. Kenny DJ, Plichta DR, Shungin D, et al. Cholesterol metabolism by uncultured human gut bacteria influences host cholesterol level. Cell Host Microbe 2020;28:245–257.e6
45. Singh V, Lee G, Son H, et al. Butyrate producers, "the sentinel of gut": their intestinal significance with and beyond butyrate, and prospective use as microbial therapeutics. Front Microbiol 2022;13:1103836
46. Guo Y, Huang Z-P, Liu C-Q, Qi L, Sheng Y, Zou D-J. Modulation of the gut microbiome: a systematic review of the effect of bariatric surgery. Eur J Endocrinol 2018;178:43–56
47. Hosomi K, Saito M, Park J, et al. Oral administration of Blautia wexlerae ameliorates obesity and type 2 diabetes via metabolic remodeling of the gut microbiota. Nat Commun 2022;13:4477
48. Murugesan S, Nirmalkar K, Hoyo-Vadillo C, García-Espitia M, Ramírez-Sánchez D, García-Mena J. Gut microbiome production of short-chain fatty acids and obesity in children. Eur J Clin Microbiol Infect Dis 2018;37:621–625
49. Yilmaz B, Mooser C, Keller I, et al. Long-term evolution and short-term adaptation of microbiota strains and sub-strains in mice. Cell Host Microbe 2021;29:650–663.e9

50. Granato A, Ryan PM, Wong A, Hamilton JK, Danska JS. Gut microbiome alterations accompany metabolic normalization following bariatric surgery in ROHHAD syndrome. JCEM Case Rep 2024;2:luae091
51. Schipper HS, Nuboer R, Prop S, et al. Systemic inflammation in childhood obesity: circulating inflammatory mediators and activated CD14++ monocytes. Diabetologia 2012;55:2800–2810
52. Petersen MC, Smith GI, Palacios HH, et al. Cardiometabolic characteristics of people with metabolically healthy and unhealthy obesity. Cell Metab 2024; 36:745–761.e5
53. Denzer C, Thiere D, Muche R, et al. Gender-specific prevalences of fatty liver in obese children and adolescents: roles of body fat distribution, sex steroids, and insulin resistance. J Clin Endocrinol Metab 2009;94:3872–3881
54. Newbern D, Gumus Balikcioglu P, Balikcioglu M, et al. Sex differences in biomarkers associated with insulin resistance in obese adolescents: metabolomic profiling and principal components analysis. J Clin Endocrinol Metab 2014;99: 4730–4739
55. Hatch-Stein JA, Kelly A, Gidding SS, Zemel BS, Magge SN. Sex differences in the associations of visceral adiposity, homeostatic model assessment of insulin resistance, and body mass index with lipoprotein subclass analysis in obese adolescents. J Clin Lipidol 2016;10:757–766
56. Gupta S, Nakabo S, Blanco LP, et al. Sex differences in neutrophil biology modulate response to type I interferons and immunometabolism. Proc Natl Acad Sci U S A 2020;117:16481–16491
57. Kautzky-Willer A, Leutner M, Harreiter J. Sex differences in type 2 diabetes. Diabetologia 2023;66:986–1002
58. Ball GDC, Huang TT-K, Gower BA, et al. Longitudinal changes in insulin sensitivity, insulin secretion, and beta-cell function during puberty. J Pediatr 2006;148:16–22
59. Pires LV, González-Gil EM, Anguita-Ruiz A, et al. The vitamin D decrease in children with obesity is associated with the development of insulin resistance during puberty: the PUBMEP study. Nutrients 2021; 13:4488